TOPICAL REVIEW — Magnetism, magnetic materials, and interdisciplinary research

Emergent phenomena in manganites under spatial confinement*

Shen Jian(沈 健)[a)b†], T. Z. Ward[c)], and L. F. Yin[a)]

[a)] State Key Laboratory of Surface Physics and Department of Physics, Fudan University, Shanghai 200433, China
[b)] Department of Physics and Astronomy, The University of Tennessee, Knoxville, TN 37996, USA
[c)] Materials Science and Technology Division, Oak Ridge National Laboratory, Oak Ridge, TN 37831, USA

(Received 29 November 2012)

It is becoming increasingly clear that the exotic properties displayed by correlated electronic materials such as high-T_c superconductivity in cuprates, colossal magnetoresistance (CMR) in manganites, and heavy-fermion compounds are intimately related to the coexistence of competing nearly degenerate states which couple simultaneously active degrees of freedom—charge, lattice, orbital, and spin states. The striking phenomena associated with these materials are due in a large part to spatial electronic inhomogeneities, or electronic phase separation (EPS). In many of these hard materials, the functionality is a result of the soft electronic component that leads to self-organization.

In this paper, we review our recent work on a novel spatial confinement technique that has led to some fascinating new discoveries about the role of EPS in manganites. Using lithographic techniques to confine manganite thin films to length scales of the EPS domains that reside within them, it is possible to simultaneously probe EPS domains with different electronic states. This method allows for a much more complete view of the phases residing in a material and gives vital information on phase formation, movement, and fluctuation.

Pushing this trend to its limit, we propose to control the formation process of the EPS using external local fields, which include magnetic exchange field, strain field, and electric field. We term the ability to pattern EPS "electronic nanofabrication." This method allows us to control the global physical properties of the system at a very fundamental level, and greatly enhances the potential for realizing true oxide electronics.

Keywords: manganites, metal–insulator transition, electrical transport, electronic phase separation

PACS: 75.25.Dk, 75.47.Gk, 73.23.–b **DOI:** 10.1088/1674-1056/22/1/017501

1. Introduction

In this new millennium, research in physics, chemistry, and life sciences is converging toward a striking commonality: understanding the physical and chemical properties of nanoscale objects. Elucidating the intricate causal relationship between fundamental interactions and length scales, and the emerging physical, chemical, or biological behavior is one of the greatest scientific and technological challenges of the 21st century. Emergent phenomena in material research, such as high temperature superconductivity, giant magnetoresistance, and quantum Hall effect, were initially discovered via controlled synthesis of novel materials with carefully tailored structure and chemical composition. While those milestone developments have defined the forefront of condensed matter science for the past twenty years, today we are presented with a golden opportunity to create nanoscale architectures using the novel tools and the rapidly expanding knowledge base of nanoscience. New research strategies aimed at connecting the world of nanophysics with complexity and emergent phenomena in artificially structured materials are a most promising avenue toward elucidating the most fundamental organizing principles of matter that may one day allow researchers to design emergent matter with desired functionality.

Correlated electronic materials (CEM) are materials with high degrees of complexity.[1–5] Colossal electroresistance, colossal magnetoresistance, high-T_c superconductivity, and multiferroicity are several fascinating emergent behaviors found in CEM; however there is yet no known theoretical model that is capable of fully explaining any one of these behaviors let alone a unifying understanding capable of explaining the effects of complexity on emergent behavior as a whole. The one thing that many of the materials exhibiting these properties share is electronic phase separation (EPS).[6] For this reason, it is imperative that we fully understand this phenomenon. Many systems with correlated electrons, such as manganites, cobaltates, and cuprates, have been shown to contain inherent electronic inhomogeneity near a phase transition. The shape and scale of EPS are different for different systems with electronic domain sizes ranging from a few nanometers to several micrometers. What is also of interest is that experimental probing and imaging techniques have suggested that there is not necessarily any preferred domain nucleation site

*Project supported by the National Basic Research Program of China (Grant No. 2011CB921801), the National Natural Science Foundation of China (Grant Nos. 91121002 and 11274071), US DOE Office of Basic Energy Sciences, Scientific User Facilities Division, and the US DOE grant DE-SC0002136, the US DOE Office of Basic Energy Sciences, Materials Sciences and Engineering Division, through the Oak Ridge National Laboratory.

†Corresponding author. E-mail: shenj5494@fudan.edu.cn

© 2013 Chinese Physical Society and IOP Publishing Ltd

under thermal cycling, which could imply that the seeding of electronic phase domains is a purely emergent phenomenon.[7] The fact that EPS is present in so many materials of such varying character raises many questions as to its origin and its role in correlated electronic systems.

Due to the strong electronic correlation in CEM, they are likely to lead to observations of striking new phenomena under spatial confinements. For instance, in transport measurements of unconfined CEM systems where the device size is larger than the inherent electronic phase domains, the current will bypass regions of high resistance in favor of regions having lower resistance, as the probing electrons will follow the path of least resistance. By reducing CEM to length scales smaller than the electronic phase domains that reside in the material, it is possible to probe both the high and low resistance domains inherent in the material using transport measurements. This method allows for a complete view of the phases residing in the material, which gives vital information on phase formation, movement, and fluctuation. Since the multiple regions also possess varied properties, this technique could lead to unexpected functionalities in future device applications. Spatial confinement of CEM exhibiting emergent phenomena is a necessary step in unlocking these systems to better scrutiny and opening them to new applications.

Ultimately, when the dimension of CEM is reduced to the length scale of the correlation length, one would expect fundamental changes of the correlated behavior. In the past, we have seen abundant evidences that simple materials become complex at small scale. For complex materials, it would be of great interest to investigate whether they become simple or even more complex when they are smaller than the correlation length scale.

Manganites are model systems to study the emergent phenomena in CEM under spatial confinements. The existence of EPS in manganites with various length scales has been widely reported,[8–13] which is also believed to have strong influences on the metal–insulator transition and the colossal magnetoresistance (CMR) in manganites.[14] If a wire could be fabricated with a width on the same scale or smaller than that expected for the EPS in the CMR materials, one would expect quite dramatic changes in functionality and the emergence of new phenomena. The challenge is that the expected length scale in most manganites is in the nanometers,[11,15] which makes the fabrication very difficult. However, submicrometer scale phase separation has been observed in the $La_{1-x}Pr_xCa_{3/8}MnO_3$ (LPCMO) system where ferromagnetic metallic and charge ordered insulating domains coexist.[16] This large-scale phase coexistence makes LPCMO an ideal model system, because wires can easily be made using the conventional lithographic fabrication processes.

In this article, we review some recent developments in studying the spatial confinement effect on manganites. The examples given are mostly based on our own results. The paper is organized as follows. After some general discussion on the experimental details of growth of manganite films and subsequent wire fabrication in Section 2, we give several examples demonstrating emergent phenomena in manganites under spatial confinement in Section 3. The attempt to control the EPS in manganites by elastic strain is described in Section 4, followed by a description of using a local external field to pattern EPS formation (termed as electronic nanofabrication) in Section 5. In the end (Section 6), we give conclusions and outlook.

2. Growth of manganite thin films and wire fabrication

Thin film epitaxial growth using laser molecular beam epitaxy (LMBE) has become one of the most popular techniques in condensed matter physics because of its versatility and relatively easy application to achieve different functionality. However, the LMBE growth process is far from simple because it involves multiple complex steps, such as ablation of target material, plasma generation and propagation through vacuum or background gas, deposition of ablated atoms on the substrate, followed by non-equilibrium processes on the surface such as diffusion, desorption, nucleation, attachment to existing atomic steps, etc.[17–19] The resulting LMBE film growth mode depends strongly on all of these steps, in addition to the consideration of the cohesive energy between the ablated atoms and the binding energy between the atoms and the substrate.[20,21] For example, the background gas pressure plays an important role on plume collision, sharpening as well as compensating film stoichiometry;[17,18] the high instantaneous deposition rate implies a high supersaturation value that gives rise to a small critical nucleus and thus high density nucleation sites;[17,18,20] temperature is known to have critical influence on the diffusion barrier, which may affect the growth mode strongly. Although various kinds of growth modes have been observed for oxide thin films under different growth conditions,[22–24] a general growth diagram that can help to guide growth control of complex oxides was not obtained till very recently.[25]

In this work, manganite thin films were grown on single crystal substrates of $SrTiO_3$, $SrLaGaO_4$, $LaAlO_3$, and $NdGaO_3$ using LMBE (248 nm, 5 Hz, 1 J/cm^2 fluence) in an ultrahigh vacuum chamber (base pressure $< 1 \times 10^{-10}$ Torr). During growth, oxygen atmosphere (8% ozone) of about 7 mTorr was used. The substrate temperature was kept at 800–900 °C to allow step flow growth, which produced thin films with high quality in terms of minimum oxygen deficiency and other structural defects. For some LPCMO thin films, the samples were immediately cooled down to room temperature after

growth and *in-situ* transferred to a scanning tunneling microscope (STM) chamber. As shown in Fig. 1, STM images confirm the existence of submicron scale EPS in the LMBE grown epitaxial films.

The high quality of the epitaxy was not only indicated by RHEED oscillations, but also verified *ex-situ* by atomic force microscopy (AFM), X-ray diffraction, and a Rutherford backscattering (RBS)/channeling experiment in a 2×1.7 MV Tandem accelerator using 2.1 MeV alpha particles (see Fig. 2). The all-important stoichiometry of the epitaxial films was further checked by comparing the phase transition point of thick films to that of the corresponding bulk.

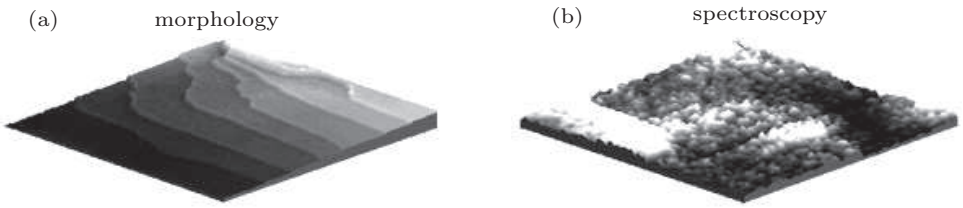


Fig. 1. The 320 nm × 320 nm topography image (a) and corresponding current image (b) simultaneously obtained from the same scanning area of 120 nm $(La_{5/8-0.3}Pr_{0.3})Ca_{3/8}MnO_3$ film at $T = 300$ K. The current image is shown for $V_{bias} = 1.6$ V.

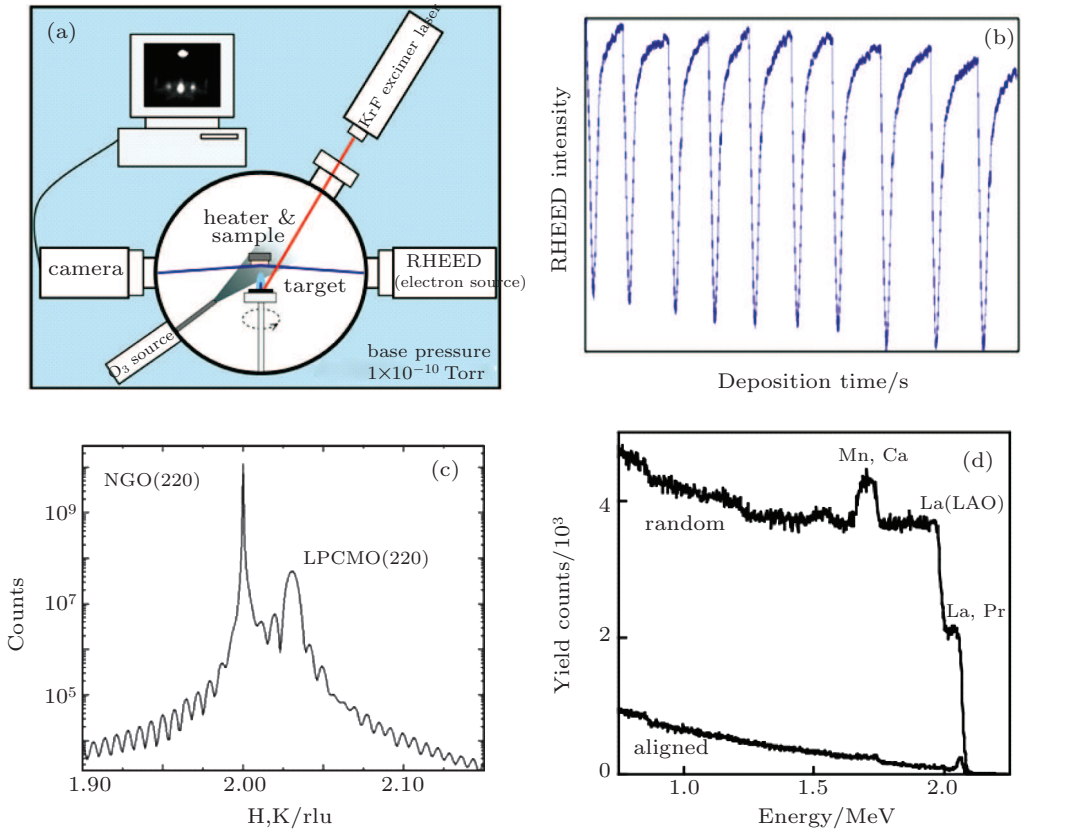


Fig. 2. Laser MBE growth of manganite films. (a) Schematic of the set-up, (b) RHEED oscillations showing unit cell by unit cell growth, (c) θ–2θ XRD scan showing fringe oscillations of a high quality film, and (d) ion channeling data indicating a minimum yield of 2% (bottom right, similar to that of single crystal Si).

For consistency, LPCMO wires of different sizes were fabricated from a single LPCMO film using optical lithography within an area of about 3 mm×3 mm, as shown by scanning electron microscope (SEM) images in Fig. 3. In every unit (∼ 0.5 mm×2.5 mm), four gold pads (gold thickness is 200 nm) have been coated onto the LPCMO film with two 500 μm×400 μm pads serving as the current contacts and two 500 μm × 200 μm pads as the voltage contacts. The electrical connections between the Au pads and the puck of a Physical Property Measurement System were made by Kulicke and Soffa wire bonders (model 4123 for Al and 4124 for Au). Twenty-micron diameter Au or Al wires were directly engaged without using any paint and solder, which removes all possible contact problems for the transport measurements. A magnetic field was applied along the easy magnetization axis, i.e., the direction perpendicular to the substrate surface during the transport measurements.

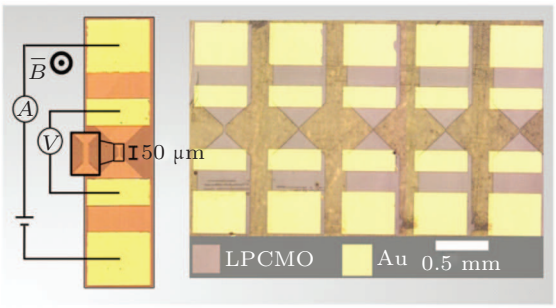


Fig. 3. SEM images of LPCMO wires fabricated from a single LPCMO/LAO(100) film with different sizes. The gold contacts are in 200 μm to 500 μm scale, which is considerably larger than the 20 μm diameter of the wire bonding thread. Current flows from top to bottom during the transport measurements.

3. Emergent phenomena in manganite wires

As mentioned earlier, the LPCMO system is well known to have coexisting ferromagnetic metal (FMM) and charge-ordered insulator (COI) domains upon its metal–insulator transition (MIT). By spatially confining epitaxial LPCMO thin films to the scales of the inherent EPS domains, the electronic transport lanes are forced to pass through both the low resistance lanes of the FMM and the high resistance lanes of the COI. This differs from past studies on bulk and thin films which probed only the low resistance lanes (Fig. 4). Through confinement, "hidden" regions are opened to scrutiny, which gives us new insight into the fundamental characteristics at play.

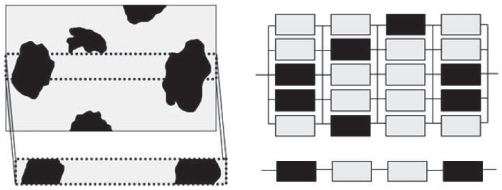


Fig. 4. Schematic diagram of film and wire with corresponding resistive networks. Black and grey areas represent FMM and COI regions.[27]

Figure 5 reveals ultrasharp jumps in resistivity of LPCMO wires on $LaAlO_3$ that become visible as the widths of the wires are reduced to a scale on the order of the inherent EPS. These jumps are attributed to a reduction of the transport lanes to a single channel. As the insulating barriers of the charge ordered state are broken by the reduction of temperature or an increase in magnetic field, the resistance in the wire shows sharp jumps around the MIT, which reflects the nature of the first-order phase transition between FMM and COI.[26]

Having established that we are capable of probing multiple domains, we are able to investigate the formation and interplay of domains. This can be accomplished by studying the effects of strain through La/Pr doping and substrate induced strain. As shown in Fig. 6, we have found a reemergent MIT that, while present, is not seen in transport measurements in either bulk or thin film form. The wire geometry forces the electronic channel to pass across both high and low resistive domains and can be modeled as a serial resistive network (Fig. 4). Further, this behavior is tunable. By varying chemical pressure and pressure from the substrate, we find that there is a critical regime in which the reemergent MIT resides, and it can be accessed through balancing these strains.[27]

Because transport measurement can reveal the signature of phase transition of an individual EPS domain in a manganite wire, it becomes possible to probe the EPS domain dynamics of manganites. This is accomplished by setting an $La_{1-x}Pr_xCa_{3/8}MnO_3$ wire at or very near the critical point of phase transition and measuring the phase fluctuation with high time resolution. The very limited number of EPS domains that can be hosted in the wire effectively removes the problems associated with spatial averaging methods in the conventional transport measurements while allowing for a high temporal resolution. At the critical point of the MIT, single domain fluctuations will show a clear signature in time-dependent resistivity measurements.

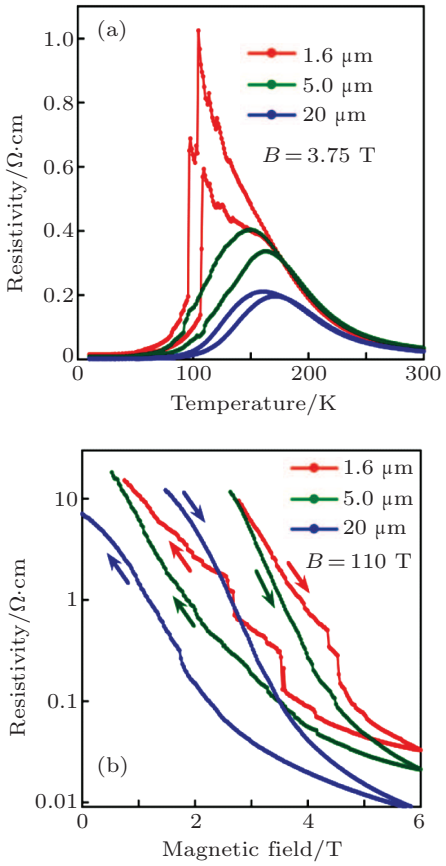


Fig. 5. (a) Resistivity versus temperature (R–T) curves for the LPCMO wires under a 3.75-T magnetic field. Arrows indicate the direction of the temperature ramp. The R–T curves all exhibit hysteresis behavior in cooling–warming cycles, which is consistent with the coexistence of FMM and COI domains in the LPCMO system. The MIT is rather smooth for both the 20 μm and the 5 μm wires. Ultrasharp and giant steps are clearly visible for the 1.6 μm wire. (b) Resistivity vs. magnetic field curves for the LPCMO wires measured at 110 K. Sudden step-like jumps are again visible in the 1.6 μm wire. Arrows indicate the sweeping directions of the magnetic field for each curve.[26]

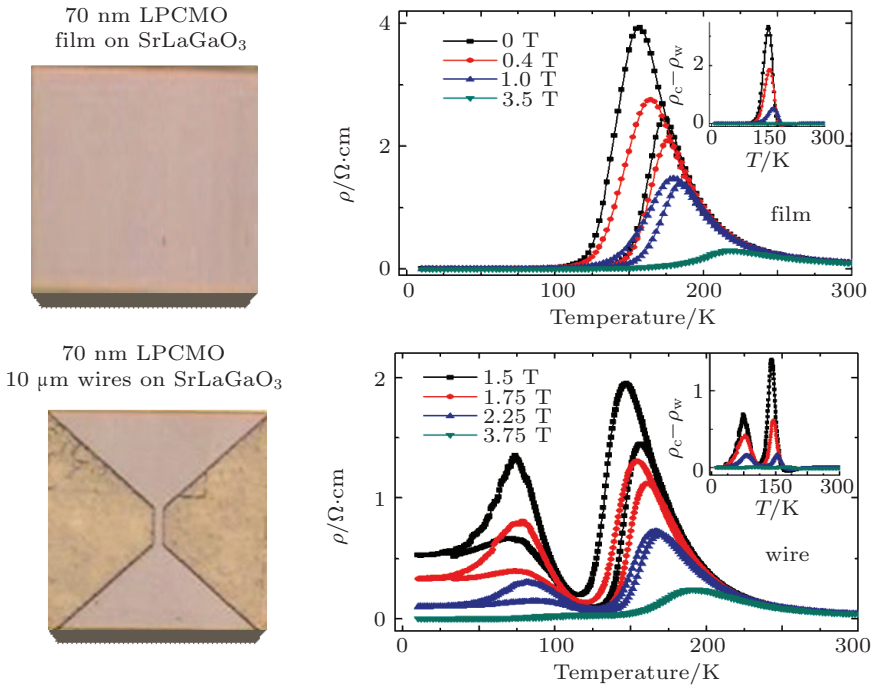


Fig. 6. Transport and magnetic properties of 70 nm $La_{0.325}Pr_{0.3}Ca_{0.375}MnO_3$ thin film and wire with $\langle r_A \rangle$ of 1.339 Å on lattice matched $SrLaGaO_4$ on heating and cooling (indicated by arrows) under increasing magnetic fields. Left: optical image of 10 mm geometry with expanded view of film (up) and wire (down). Upper right: comparison of temperature dependence of resistivity in film at 0 T (black), 0.4 T (red), 1 T (blue), and 3.5 T (green). The film shows a single MIT peak. Lower right: comparison of temperature dependence of resistivity in 10 μm wire at 1.5 T (black), 1.75 T (red), 2.25 T (blue), and 3.75 T (green). The wire shows a reemergent, low temperature peak in r that is not present in the film. Insets show differences in resistivity between warming and cooling curves.[27]

Figure 7(a) shows resistivity of 10 μm×50 μm×70 nm LPCMO wire as a function of temperature on warming under a 3.75 T magnetic field. This field is sufficient to align the ferromagnetic domains without melting the charge ordered phase, which allows us to probe only the electronic domains without the interference from magnetic domains. The MIT is clearly visible across a 2 K window centered at 83 K as an ultrasharp peak in resistivity (ρ) with a $\Delta\rho/\rho$ of 3200%. This is contrasted with the same sample in a film geometry (Fig. 7(a) inset), which shows a smooth transition from metallic to insulating behavior across a 150 K window. Figures 7(b) and 7(c) show the time-dependent resistivity while the wire is held at the transition temperature. Figure 7(b) has a relatively low time resolution of 10 s and is characterized by a stable competition between two states with resistivity jumps of 46%. By increasing the time resolution from 10 s to 22 μs, the true nature of this volatility becomes clear (Fig. 7(c)). The apparent two-state system is actually comprised of a much richer multistate system. There are three inherent resistivity levels, each containing a further two-state fluctuation. In contrast, the film (Fig. 7(c) inset) only exhibits white noise. These fluctuations in the wire are a direct signal of the microscopic fluctuations in EPS domains at the transition temperature.[28]

As shown above, confining a thin film to a wire allows us to gather high resolution dynamical information on a single or few electronic domains residing in the wire as they transition between insulating and metallic phases. The behavior and response of a first-order phase transition have not been well studied in the previous works, but as we seek to better understand the mechanisms that drive electronic phase transitions and begin to incorporate these materials in practical devices, such as in magnetic cooling or memory applications, it is vital to investigate the timescales at which these transitions occur.

The data collected in Fig. 7 is further investigated as it contains a single two-state fluctuation that is present in three background states. This allows us to study the influence of background effects on a single electronic domain's dynamics.[29] Figure 8(a) shows a snapshot of the time-dependent resistance of the 10 μm wide wire held at the critical point of 83 K under a 3.75 T magnetic field. We see that within each of the three background levels, there is a single active domain that can be observed. This means that any differences in this single domain's dynamics can be directly attributed to changes in the applied electric field arising from background resistive changes, local current effects as the resistive network is modified, and correlations between neighboring domains as they undergo transition. We interpret the high and the low resistance states as arising from a single phase domain set in a complex switching network dominating the transport signal as it transitions between the FMM phase and the COI phase. The inset shows a typical transition from the FMM phase to the COI phase followed a few milliseconds

later by a transition back to the FMM phase.

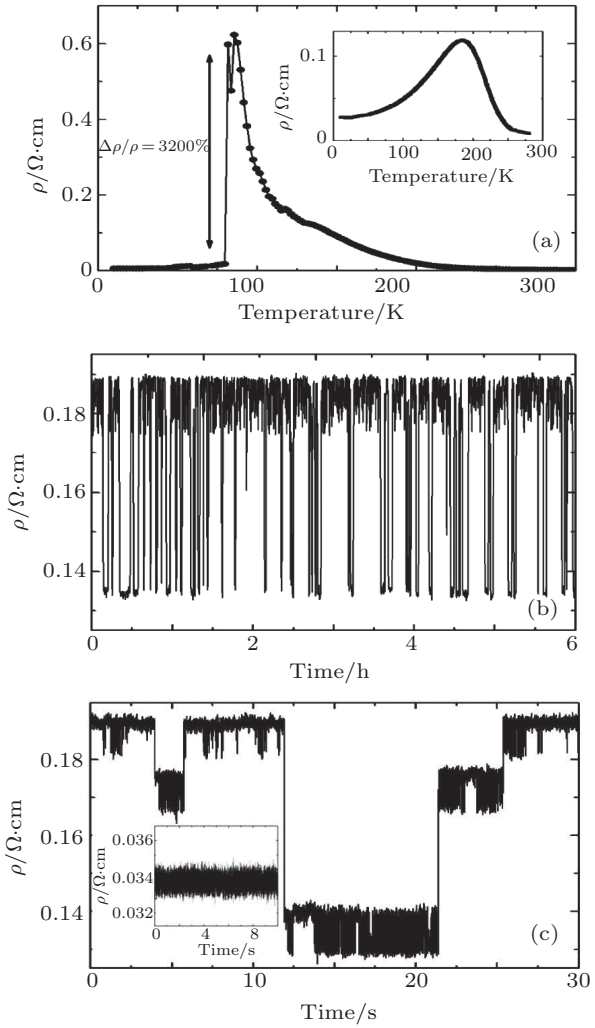


Fig. 7. Transport measurements. (a) Temperature dependent resistivity plot for a 10 μm wide LPCMO wire under 0.5 μA constant current (inset: temperature vs. resistivity plot of the same sample in a thin film form.) (b) Long scale, low sample frequency resistivity vs. time plot for wire held at 83 K. (c) Wire's resistivity vs. time plot at the transition temperature taken at a sampling frequency of 45 kHz Inset: film's resistivity vs. time plot under the same conditions. [28]

To find the lifetime of the single electronic domain as it undergoes transition, we use an inverse exponential fitting $R = A\,e^{-t/\tau}$, where R is the resistance, A is a constant, t is time, and τ is the transition lifetime. Thousands of transitions on the 3 levels were fitted; the results of which are shown in Fig. 8(b) with the error bars representing the standard deviation in fitted lifetimes. The first thing that we can observe is that the metallic to insulating transition time is consistently longer than the insulating to metallic transition time. This could be a response to the disordered FMM phase requiring a longer time to order itself into the COI phase than that for the COI phase to disorder to FMM. The observed transition times are on the order of milliseconds, which is several orders longer than what would be expected for a purely quantum electrical transition or from the thermal dissipation resulting from the free energy release.[30,31] This longer transition time may be the signature of an intermediate glassy phase and is quite different from the nanoseconds transitions that have been induced using vibrational excitations[32] or the femtoseconds to picoseconds transitions induced through photo excitations.[33] These short-time transitions have been described as forced transitions where the probing excitation directly separates and melts the charge/orbital order parameters from the larger system.[34] This is an important point, as it suggests that phase transitions that are driven by an external stimulation push the systems far out of equilibrium, so they should not be considered when trying to understand the dynamics of a phase transition at a stable critical point.

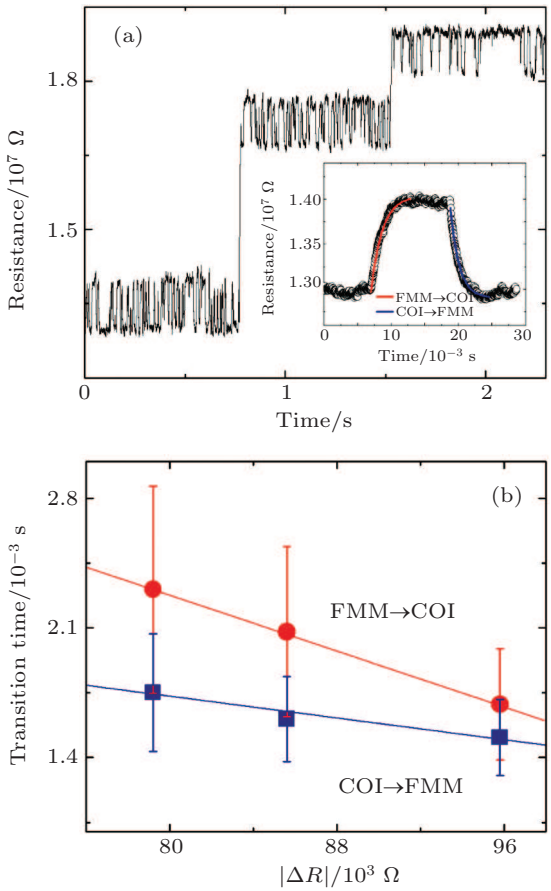


Fig. 8. (a) LPCMO wire held at a critical point where a single small domain's phase transitions can be tracked across 3 different background resistive states due to modifications of the transport channel away from the domain site. (Inset) Typical two-state fluctuation that is observable on each of the three levels. Lines indicate type of transition that the small domain is undergoing. (b) Transition times of a single electronic domain on each of the 3 background states. Error bars denote standard deviation. These lifetimes are taken from thousands of individual transitions on each of the 3 background resistive states. In each case, it takes longer for the domain to transition from the disordered FMM phase to the ordered COI phase.[29]

4. Control electronic phase separation by epitaxial strain

In a previous section, we demonstrated that EPS in manganites can lead to striking phenomena when the system is

confined to a dimension comparable to the size of EPS. Moreover, the spatial confinement also offers a mean to study the dynamic behavior of an individual EPS domain, which is generally very challenging using any existing imaging techniques. In this section, we will discuss the first attempt to control the process of EPS formation, which allows us to tune the global physical properties of the system.

In the past, inherent crystalline strain and local lattice distortions have been known to have a strong influence over the formation of EPS.[35–37] Combining these influences, theoretical models based on electronic and elastic degrees of freedom have shown that a large scale EPS can self-organize into elongated domains with no preference for uniaxial orientation.[35] By applying an anisotropic long range strain field to an EPS system, we can investigate the specific effects of elastic energy on the emergent formation of coexisting EPS domains. We again use $La_{5/8-x}Pr_xCa_{3/8}MnO_3$ ($x = 0.3$) as a model system and compare the transport data of two perpendicular in-plane directions in the case of an anisotropically strained orthorhombic structure. While other methods, such as magnetic force microscopy (MFM)[38–40] and out-of-plane vs. in-plane transport,[41] have found evidences of local variation in domain formation due to strain effects, the ability of in-plane vs. in-plane transport measurements to identify the percolation point in metal–insulator transitions on global levels makes it the ideal method for understanding how emergent EPS affects macroscopic properties such as CMR and the metal–insulator transition.

While bulk LPCMO is a pseudocubic perovskite at room temperature, we are able to force a 50-nm LPCMO thin film to epitaxially conform to the in-plane lattice parameters of an orthorhombic $NdGaO_3$ (NGO) substrate.[42] The in-plane lattice commensurability induces anisotropic, tensile strain fields in the epitaxial film. For comparison, we have also grown a 50-nm LPCMO film on an $SrLaGaO_4$ (SLGO) substrate, which is tetragonal with in-plane lattice parameters less than 0.1% different from those of the bulk LPCMO.

In Fig. 9(a), the direction-dependent resistivity on heating and cooling as a function of temperature under a 7.5-T magnetic field is examined for a 50-nm thick LPCMO film on NGO. Transport is shown along the two in-plane directions corresponding to the $[10\bar{1}]$ and [101] directions (Fig. 9(b) inset). Remarkably, the MIT temperature (T_{MIT}) measured along the more strained $[10\bar{1}]$ direction is 24 K higher than that measured along the [101] direction. The difference between the resistivities measured at the respective T_{MIT} is 0.31 Ω·cm, which corresponds to a relative variation of ∼200%. In fact, the anisotropic resistivity, i.e., relative difference in resistivities compared at the same temperature ($(\rho_{[101]} - \rho_{[10\bar{1}]})/\rho_{[10\bar{1}]}$), is even larger, reaching 500% at 110 K (Fig. 9(b)). Interestingly, in the temperature range between the two T_{MIT}s, the system acts as a metal in the $[10\bar{1}]$ direction and an insulator in the [101] direction. In contrast, figure 9(c) shows the temperature dependent resistivity for the 50-nm LPCMO film grown on an SLGO (001) substrate. Comparing the in-plane transport curves, we see that there is a relative variation of only ∼1%

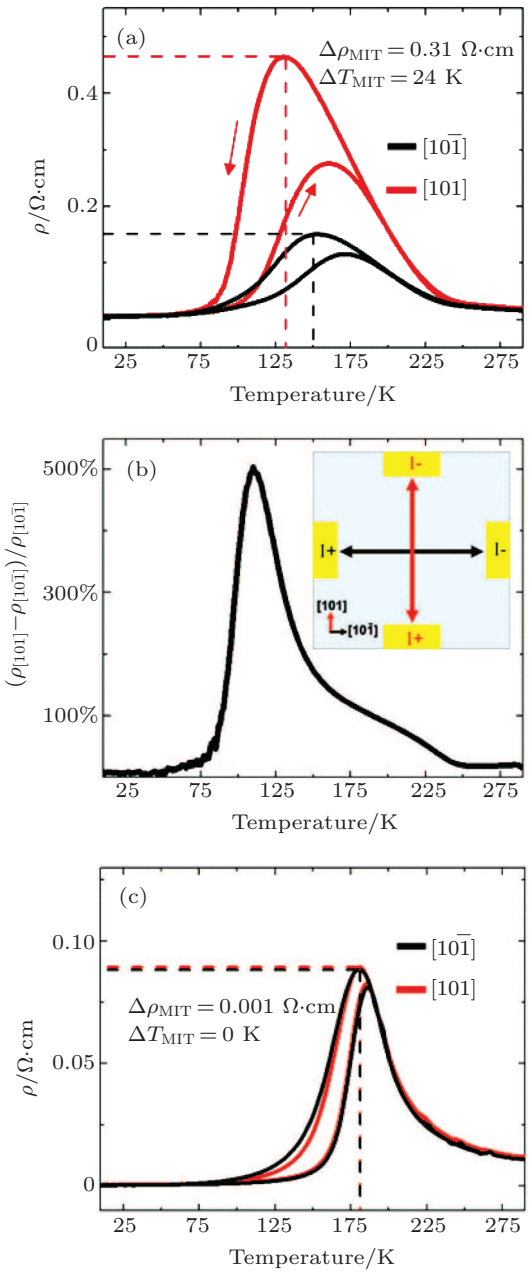


Fig. 9. In-plane transport properties. (a) LPCMO film on an NGO substrate has anisotropic in-plane strain and shows significant differences in both the MIT temperature and the resistivity at the MIT depending on which axis transport is taken across. (b) Relative percent difference between cooling curves along perpendicular in-plane directions for LPCMO on NGO. Inset: diagram showing directions of transport in the LPCMO thin film relative to the in-plane axes. (c) LPCMO film on an SLGO substrate has isotropic in-plane strain and shows negligible differences in transport along the two in-plane axes. Note that for panel (c), the strain field along [101] = the strain field along $[10\bar{1}]$, while in panel (a), the strain field along [101] < the strain field along $[10\bar{1}]$.[42]

in the resistivity at the MIT and that there is no difference in T_{MIT}. This strongly suggests that the anisotropic strain field applied by the NGO substrate must be the driving mechanism for the observed differences.

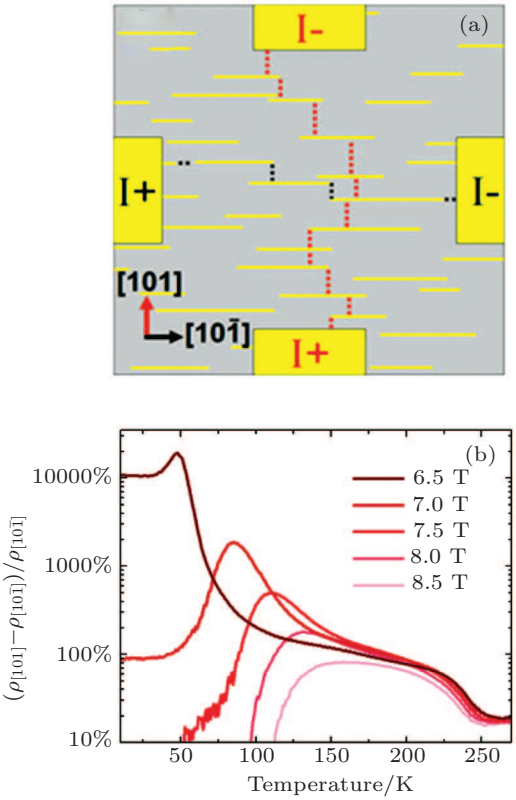


Fig. 10. Effects of anisotropic strain field applied through NGO substrate on LPCMO film. (a) Diagram of a percolative model in which the metallic phase domains have an elongated aspect ratio directed along axis under the higher strain field. Yellow lines indicate randomly seeded regions of low resistance laid in a high resistance background. Dotted lines indicate possible high resistance channels through which current must travel in each direction. (b) Resistivity percent difference between orthogonal in-plane cooling curves is maximized at low field.[42]

Because the MIT in the LPCMO system is percolative in nature, the higher T_{MIT} along the strained [10$\bar{1}$] direction indicates that there is a preferential seeding and growth of FMM domains along the [10$\bar{1}$] direction, which is determined to be the easy magnetization axis. Figure 10(a) presents an illustration of how the elongated domains act to channel the current, which leads to a higher T_{MIT} along the [10$\bar{1}$] direction. In an insulating background with preferentially elongated metallic domains oriented along one direction, the measured resistivity in line with the metallic domains will be substantially lower. As a matter of fact, the anisotropic resistivity is extraordinarily high in this system (Fig. 10(b)). For instance, the anisotropic resistivity reaches ~20000 % at 48 K under a 6.5 T field. With increased magnetic field, this difference is reduced. This is because the melting of the COI phase by the magnetic field destroys the elongated aspect ratio of the metallic domains, which means that the current path along the [101] direction is no longer dominated by the insulating regions. This behavior also allows for magnetic field tunable anisotropic resistivity.

The large anisotropic transport behavior of the LPCMO system under the presence of an anisotropic strain field indicates that the EPS depends sensitively on the long-range elastic strain. We have shown that the formation and the orientation of EPS domains can be guided by applying a uniaxial strain field. Even within the same plane, the metallicity can change drastically along different directions with respect to that of the strain field. Consequently, the system exhibits extraordinarily large anisotropic resistivity, which can, in turn, be used to detect subtle changes in the external strain field from the environment. These findings show that emergent EPS domain formation can be selectively tuned over long distances, which opens the door to engineering novel devices and to understanding more fully the balanced energetics that drive emergent behaviors in CEM.

5. Electronic nanofabrication of manganites

For most CMR manganites, both the MIT and the amplitude of magnetoresistance critically depend on the percolation of FMM domains in the system. Controlling the formation and the spatial distribution (size, density, symmetry, etc.) of the electronic domains will not only help to understand the origin of the electronic phase separation, but also help to design manganites or other CEM materials with desired properties for all-oxide based electronic devices.

The key to achieving control of the formation and the spatial distribution of electronic domains in manganites is a novel method called electronic nanofabrication, a conceptually new approach. In striking contrast to the conventional nanofabrication, the electronic nanofabrication patterns electronic states in materials without changing the actual size, shape, and chemical composition of the materials. Specifically, we will use local external fields to drive a local electronic phase transition and eventually control the formation and the spatial distribution of electronic states by patterning the local external fields. The success of this approach will open a new avenue to designing physical properties in CEM.

Our recent work has shown that the electronic nanofabrication is a promising method for manganites.[42] Figure 11 shows that by growing magnetic Fe nanodots on the surface of a 20 nm thick $La_{0.7}Ca_{0.3}MnO_3/LaAlO_3(001)$ film, we have turned the film from an insulator to a metal with a high MIT temperature. The underlying mechanism is understood to be the local magnetic exchange field between Fe and Mn spins that aligns the local Mn spins leading to the formation of a local metallic state. As shown in Fig. 12, the MIT temperature is tunable by the density of Fe nanodots, which strongly indicates that the local metallic state follows the spatial locations of the Fe nanodots.

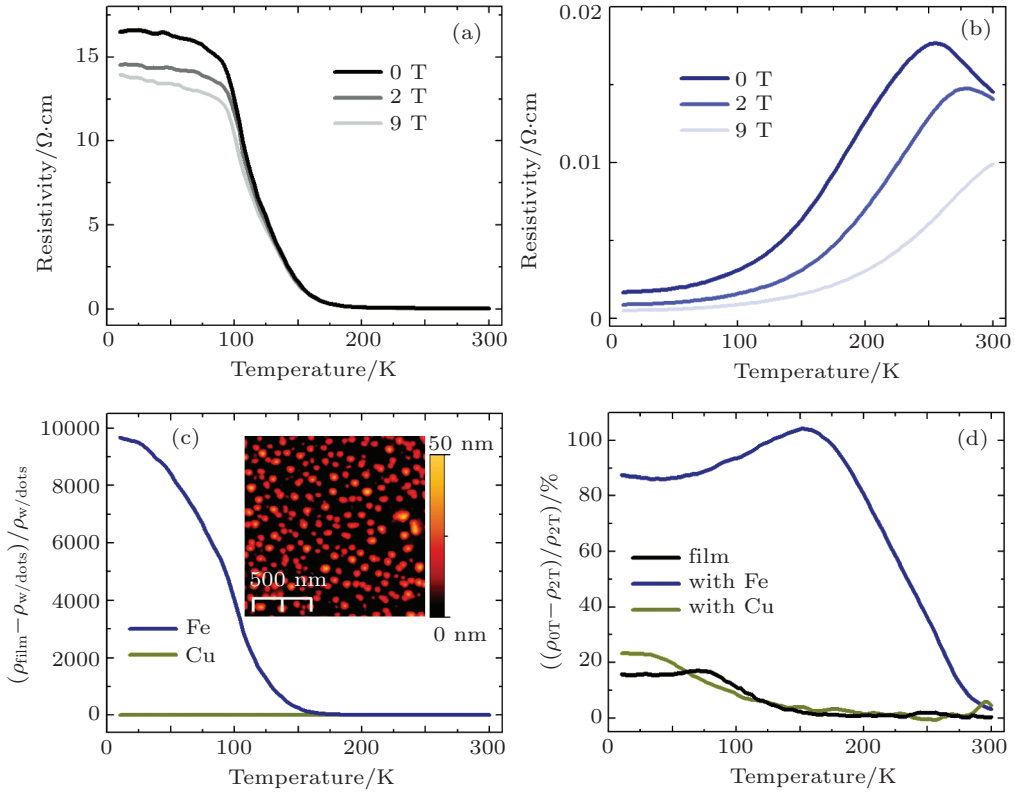


Fig. 11. Transport properties of ultrathin LCMO film before and after application of nanodots. (a) Resistivity behavior for 20 nm ultrathin film of $La_{0.7}Ca_{0.3}MnO_3$ showing insulating behavior and no clear metal–insulator transition. (b) Resistivity data of the same film after applying Fe nanodots to surface showing a recovery to bulk-like behavior with an MIT temperature of 255 K at 0 T (note change in scale). (c) Ferromagnetic Fe nanodots drive a huge change in the film's resistivity compared to the diamagnetic Cu nanodots. Insets: AFM images of typical nanodot coverages for Cu and Fe systems on LCMO films. (d) Magnetoresistive behavior shows a much higher magnetic response in the spin coupled system.[43]

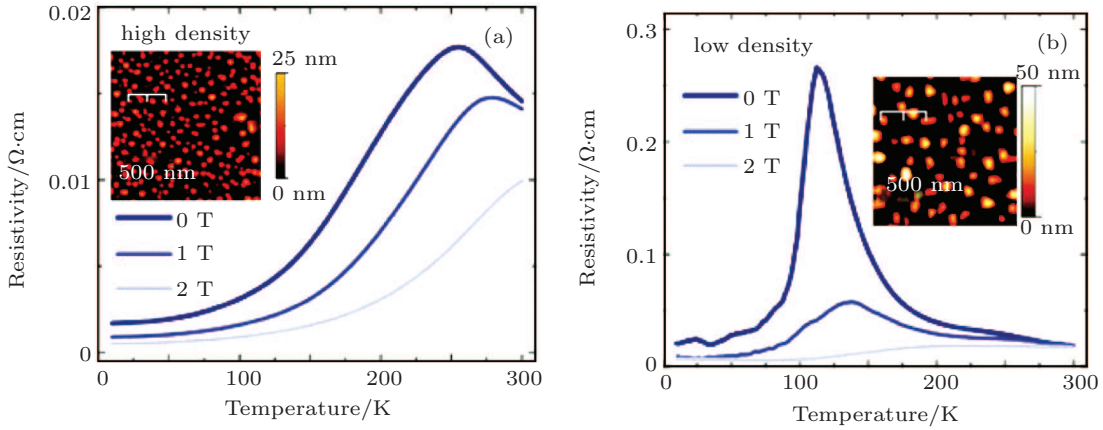


Fig. 12. Comparison of transport properties with different Fe nanodot density. Resistive data for an ultrathin LCMO film after application of low density Fe nanodots shows recovery of the metal–insulator transition but with a much lower transition temperature than that seen at higher nanodot densities.[43]

Besides the magnetic exchange field, many other external fields can influence the electronic states of CEM. These include magnetic fields, electric fields, strain fields, and electromagnetic fields induced by short-wavelength light. Our very recent work indicates that a local electric field can be used to tune the transport behavior of manganites wires as well.[44]

To carry out electronic nanofabrication using these external fields, one needs to resolve the following three issues. (i) When an external field is confined to the nanometer scale and applied to a CEM sample, can a local electronic phase transition occur? If yes, what are the stability and the dimensions of the transformed electronic state? (ii) When the local external fields are patterned into a designed symmetry with changing size and shape, will the transformed electronic states follow their pattern? (iii) Can we use imaging methods to provide information on the electronic, spin, and lattice structures of the

transformed electronic states?

Focusing on these issues, manganite thin films can be used as model systems for electronic nanofabrication. The developed electronic nanofabrication methods can then be applied to spatially confined manganites such as wires and dots, which will enhance the response of the system to the external fields. Other CEM materials including multiferroic materials will also be used for electronic nanofabrication in the future. Figure 13 shows some of the possible routes to carry out electronic nanofabrication for manganites.

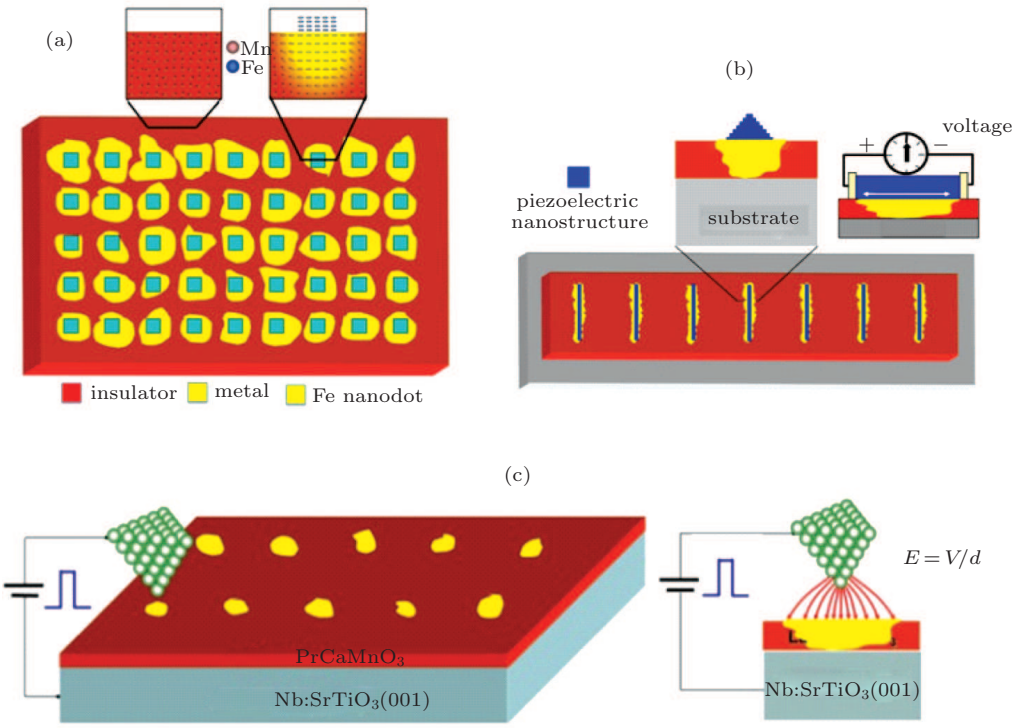


Fig. 13. (a) Schematic picture of an assembly of patterned Fe nanostructures on a manganite thin film surface. (b) Schematic picture of patterned epitaxial piezoelectric nanostructures on a manganite thin film surface. The tunable local strain field is applied due to lattice misfit between the piezoelectric and manganite. (c) Local electric field induced by voltage pulse from SPM tip. A designed pattern can be written using the tip.

6. Concluding remarks

For condensed matter physicists, materials are often separated into two classes: simple materials and strongly correlated materials. Because the interesting problems in these fields of study are very different, there is traditionally very little overlap between the two. However, in the world of reduced dimensionality, the line is no longer well defined. Simple materials can become complex, and complex materials can become even more complex, or, sometimes, simple. In this paper, we have used CMR manganites as a model system to demonstrate how emergent phenomena appear in reduced dimensionality. The emergent phenomena mostly originate from the EPS in the manganite system. Helped by the spatial confinement, the nature of the EPS including their dynamics can be cleanly studied using the conventional transport measurements. It is hoped that such work will lead to a new field where the interplay between complexity and quantum effects will generate fascinating new properties for future technology.

References

[1] The April 21st Issue of *Science* **288** (2000) was dedicated to correlated electron systems.
[2] Chu Y H, Martin L W, Holcomb M B and Ramesh R 2007 *Mater. Today* **10** 16
[3] Israel C, Calderón M J and Mathur N D 2007 *Mater. Today* **10** 24
[4] Habermeier H 2007 *Mater. Today* **10** 34
[5] Ohta H 2007 *Mater. Today* **10** 44
[6] Moreo A, Yunoki S and Dagotto E 1999 *Science* **283** 2034
[7] Shenoy V B, Sarma D D and Rao C N R 2006 *ChemPhysChem* **7** 2053
[8] Zhang L W, Israel C, Biswas A, Greene R L and de Lozanne A 2002 *Science* **298** 805
[9] Loudon J C, Mathur N D and Midgley P A 2002 *Nature* **420** 797
[10] Ma J X, Gillaspie D T, Plummer E W and Shen J 2005 *Phys. Rev. Lett.* **95** 237210
[11] Tao J, Niebieskikwiat D, Varela M, Luo W, Schofield M A, Zhu Y, Salamon M B, Zuo J M, Pantelides S T and Pennycook S J 2009 *Phys. Rev. Lett.* **103** 97202
[12] Murakami Y, Kasai H, Kim J J, Mamishin S, Shindo D, Mori S and Tonomura A 2010 *Nat. Nanotech.* **5** 37
[13] Lai K J, Nakamura M, Kundhikanjana W, Kawasaki M, Tokura Y, Kelly M A and Shen Z X 2010 *Science* **329** 190
[14] Dagotto E, Hotta T and Moreo A 2001 *Phys. Reports* **344** 1
[15] Salamon M and Jaime M 2001 *Rev. Mod. Phys.* **73** 583
[16] Uehara M, Mori S, Chen C H and Cheong S W 1999 *Nature* **399** 560
[17] Chrisey D B and Hubler G K 1994 *Pulsed Laser Deposition of Thin Films* (New York: Wiley)

[18] Willmott P R and Huber J R 2000 *Rev. Mod. Phys.* **72** 315
[19] Shen J, Gai Z and Kirschner J 2004 *Surf. Sci. Report* **52** 163
[20] Willmott P R 2004 *Progress in Surface Science* **76** 163
[21] Ashfold M N R, Claeyssens F, Fuge G M and Henley S J 2004 *Chem. Soc. Rev.* **33** 23
[22] Hong W, Lee H N, Yoon M, Christen H M, Lowndes D H, Suo Z and Zhang Z 2005 *Phys. Rev. Lett.* **95** 95501
[23] Ohtomo A and Hwang H Y 2007 *J. Appl. Phys.* **102** 83704
[24] Sinha S K, Bhattacharya R, Ray S K and Manna I 2011 *Mater. Lett.* **65** 146
[25] Guo H W, Sun D, Wang W, Gai Z, Kravchenko I, Shao J, Jiang L, Ward T Z, Snijders P C, Yin L F, Zhang Z, Shen J and Xu X S *Growth diagram of $La_{0.7}Sr_{0.3}MnO_3$ Thin Films using Pulsed Laser Deposition* (submitted to *J. Appl. Phys.*)
[26] Zhai H Y, Ma J X, Gillaspie D T, Zhang X G, Plummer E W and Shen J 2006 *Phys. Rev. Lett.* **97** 167201
[27] Ward T Z, Liang S H, Fuchigami K, Yin L F, Dagotto E, Plummer E W and Shen J 2008 *Phys. Rev. Lett.* **100** 247204
[28] Ward T Z, Zhang X G, Yin L F, Zhang X Q, Liu M, Snijders P C, Jesse S, Plummer E W, Cheng Z H, Dagotto E and Shen J 2009 *Phys. Rev. Lett.* **102** 087201
[29] Ward T Z, Gai Z, Guo H W, Yin L F and Shen J 2011 *Phys. Rev.* B **83** 125125
[30] Quintero M, Sacanell J, Ghivelder L, Gomes A, Leyva G and Parisi F 2009 *Physica* B: *Condensed Matter* **404** 2763
[31] Lima Sharma A, Sharma P, McCall S, Kim S and Cheong S 2009 *Appl. Phys. Lett.* **95** 092506
[32] Rini M, Tobey R, Dean N, Itatani J, Tomioka Y, Tokura Y, Schoenlein R W and Cavalleri A 2007 *Nature* **449** 72
[33] Polli D, Rini M, Wall S, Schoenlein R W, Tomioka Y, Tokura Y, Cerullo G and Cavalleri A 2007 *Nat. Mater.* **6** 643
[34] Ogasawara T, Kimura T, Ishikawa T, Kuwata-Gonokami M and Tokura Y 2001 *Phys. Rev.* B **63** 113105
[35] Ahn K H, Lookman T and Bishop A R 2004 *Nature* **428** 401
[36] Gillaspie D, Ma J X, Zhai H Y, Ward T Z, Christen H M, Plummer E W and Shen J 2006 *J. Appl. Phys.* **99** 08
[37] Dhakal T, Tosado J and Biswas A 2007 *Phys. Rev.* B **75** 092404
[38] Wu W, Israel C, Hur N, Park S, Cheong S W and de Lozanne A 2006 *Nat. Mater.* **5** 881
[39] Dho J, Kim Y N, Hwang Y S, Kim J C and Hur N H 2003 *Appl. Phys. Lett.* **82** 1434
[40] Zhang L, Israel C, Biswas A, Greene R L and de Lozanne A 2002 *Science* **298** 805
[41] Rairigh R P, Singh-Bhalla G, Tongay S, Dhakal T, Biswas A and Hebard A F 2007 *Nat. Phys.* **3** 551
[42] Ward T Z, Budai J D, Gai Z, Tischler J Z, Yin L F and Shen J 2009 *Nat. Phys.* **5** 885
[43] Ward T Z, Gai Z, Xu X Y, Guo H W, Yin L F and Shen, J 2011 *Phys. Rev. Lett.* **106** 157207
[44] Guo H W, Noh J H, Dong S, Rack P D, Gai Z, Xu X, Dagotto E, Shen J and Ward T Z *Dynamic Resistive Switching Controlled by Local Lateral Gating in Phase Separated Manganite Wires* (submitted to *Nature Comm.*)